Remote Sensing of Environment 235 (2019) 111441

Contents lists available at ScienceDirect

Remote Sensing of Environment

journal homepage: www.elsevier.com/locate/rse

Spatio-temporal pattern of soil degradation in a Swiss Alpine grassland catchment

Lauren Zweifel[a,*], Katrin Meusburger[b], Christine Alewell[a]

[a] Department of Environmental Science, University of Basel, Bernoullistrasse 30, 4056 Basel, Switzerland
[b] Swiss Federal Research Institute WSL, Zürcherstrasse 111, 8903 Birmensdorf, Switzerland

ARTICLE INFO

Keywords:
Shallow landslides
Sheet erosion
Orthophotography
Time series
Object-based image analysis
Mapping
Alps

ABSTRACT

Soil degradation on Alpine grasslands is triggered mainly by extreme topography, prevailing climate conditions and land use practices. Suitable monitoring tools are required to assess soil erosion with high temporal and spatial resolution. In this study, we present an unprecedented and comprehensive approach based on object-based image analysis (OBIA) to map and assess all occurring erosion processes within a catchment (Urseren Valley, Switzerland). Five high-resolution (0.25–0.5 m) orthophotos with RGB spectral information (SwissImage) produced during a 16-yr period were analyzed. Soil erosion sites are classified according to their type (shallow landslide or sites with reduced vegetation cover affected by sheet erosion) or the triggering land use management impacts (haying, trampling) with the Overall Accuracy ranging between 78 and 88% (Kappa 0.65–0.81) for the different years. The area affected by soil erosion increases for all classes during the study period (2000–2016) by a total of 156 ± 18% (increase consisting of 3% shallow landslides, 5% livestock trails, 46% sheet erosion and 46% management effects). Slopes at lower elevations (< 1800 m asl) are increasingly affected by livestock trails and sheet erosion caused by trampling and grazing as well as other management practices. For areas located above the agricultural land use, an increase in shallow landslides, as well as sheet erosion, can be observed. This points to climate change as a triggering factor of soil degradation, which has not been identified so far as a factor for soil erosion in the Urseren Valley. While OBIA yields conservative estimations mainly due to limitations of spatial resolutions, the method facilitates a comprehensive overview of the ongoing temporal and spatial development regarding soil degradation within the Urseren Valley.

1. Introduction

Alpine grasslands can be strongly affected by various types of soil erosion triggered by wind, water, snow, gravity and management impacts (e.g., trampling). Future climate change is expected to have a strong impact on the Alpine region causing not only an increase in temperature but also a change in frequency and intensity of precipitation events as well as strongly altered snow dynamics (Beniston, 2006, 2012; CH2011, 2011; Frei et al., 2018; CH2018, 2018). Along with changing land use practices, such as intensified use of pastures, these changes are expected to have an increasing effect on the soil erosion rates in Alpine regions (Bosco et al., 2009; Meusburger and Alewell, 2008, 2009; Scheurer et al., 2009). Certain Alpine regions already experience high rates of soil erosion (e.g., average erosion rate of 180 t km^{-2} yr^{-1} with a maximum in erosional hot spots of 3000 t km^{-2} year^{-1} in the Urseren Valley) and thereby exceed Alpine soil production rates (for old soils between 54 t km^{-2} yr^{-1} and 113 t km^{-2} yr^{-1}, for young soils between 119 t km^{-2} yr^{-1} and 248 t km^{-2} yr^{-1})(Alewell et al., 2015). In combination with the extreme prevailing topographic and climate conditions, the land use can be considered unsustainable (Meusburger and Alewell, 2014). The main types of erosion processes occurring in our study area (Urseren Valley, Central Swiss Alps) are landslides, sheet erosion (e.g., rill and inter-rill erosion), livestock trails and damages due to management (i.e., haying, use of heavy machinery, over-fertilisation). We separate livestock trails from other management effects due to the very different appearances, triggering factors and distribution in the catchment.

Shallow landslides typically have a size of 2–200 m^2 and occur when a triggering event, such as heavy and prolonged precipitation or movement of the snow cover displaces the topsoil layer (Ceaglio et al., 2012; Wiegand and Geitner, 2010a; b). In many cases it is a combination of both triggers which eventually lead to landslides (e.g., disturbance of surface stability by the snow, then water saturation with heavy rain events). These areas continue to be exposed to further

* Corresponding author.
E-mail address: lauren.zweifel@unibas.ch (L. Zweifel).

https://doi.org/10.1016/j.rse.2019.111441
Received 4 April 2019; Received in revised form 19 August 2019; Accepted 23 September 2019

erosion by wind and water and might take years to decades to re-vegetate or might even steadily increase. While shallow landslides are a naturally occurring phenomenon, pasture management (e.g., trampling by livestock, stocking density) can have a destabilizing effect, increasing the local susceptibility to landslides (Maag et al., 2001; Meusburger and Alewell, 2008; Schauer, 1975; Tasser and Tappeiner, 2002). Sheet erosion is the result of surface run-off and the consequent detachment and displacement of topsoil particles down slope (Alewell et al., 2019; Nearing et al., 2017). Sheet erosion can affect large areas and occur for long periods of time before being noticed. Livestock trails are the direct result of trampling by livestock, when the vegetation cover has not enough time for recovery and the soil is compacted (Apollo et al., 2018). These trails mainly develop in pasture areas following the contour lines of the slope, when livestock traverse steep areas. The reduction of vegetation cover through trampling and overgrazing can increase sheet erosion.

Scientific communities working on the different phenomena of soil erosion are often separated due to the varying methods applied to capture these erosion processes (e.g., field measurements, mapping, modeling or tracer techniques). However, erosion processes interact and boundaries are not clear between the processes and may be overlapping. Local authorities need information on the overall soil degradation situation, which is impossible to achieve from surveys at ground level in the field. Here, remote sensing offers the opportunity to observe and monitor different erosion processes at high spatial resolutions. This might set the methodological framework to study spatio-temporal auto-correlation between different erosion processes and will extend the study of susceptibility mapping beyond landslides to other processes of soil degradation.

All above mentioned erosion processes can be observed on high-resolution orthophotos (Fig. 1). While many changes have occurred over the course of 16 years, such as the general vegetation cover (e.g., reduction of shrubs), an increase in bare soil sites as well as a reduction of the vegetation cover in certain areas is evident. A photograph taken in 2009 shows the severity of these erosion features in the field (Fig. 2). As object-based image analysis (OBIA) has proven to be a reliable tool for many difficult detection tasks in the field of remote sensing, especially in the case of high-resolution images (pixel size < object size) (Blaschke, 2010; Chen et al., 2018), our hypothesis is, that in spite of very different color ranges and brightness between photos, temporal development of degradation features can be mapped.

When applying this semi-automated method, the pixels of remotely sensed images are first grouped into segments producing image objects containing pixels with similar spectral properties. The image objects are then classified based on the information associated with the objects, such as spectral, spatial, textural or contextual properties (Martha et al., 2010, 2012; Stumpf and Kerle, 2011). In the case of soil erosion, OBIA has been extensively used to map landslides on satellite images, mainly with the aim of producing landslide inventory maps (Eisank et al., 2014; Guzzetti et al., 2012; Hölbling et al., 2015, 2016a, 2017; Martha et al., 2012; Mayr et al., 2016; Stumpf and Kerle, 2011; Wiegand et al., 2013). In some studies, aerial images were used for mapping purposes instead of or in addition to satellite images (Hölbling et al., 2016a, b; Moine et al., 2009). Other applications of OBIA for capturing soil erosion consist of rill and gully erosion mapping (D'Oleire-Oltmanns et al., 2014; Johansen et al., 2012; Karami et al., 2015; Shruthi et al., 2011, 2014, 2015). Gully erosion is not assessed in this study, as it does not occur on grassland in our catchment, but might be captured with the technique in other areas.

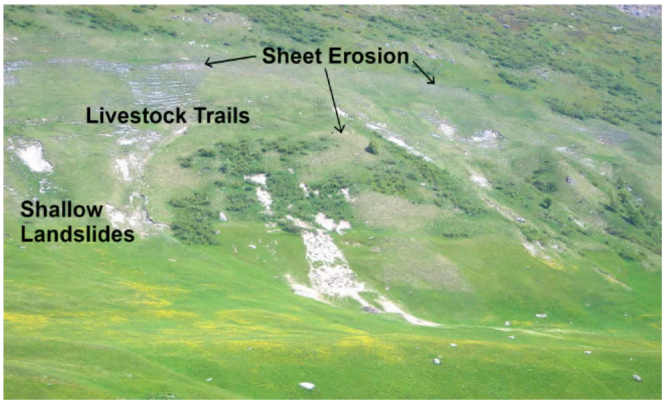

Fig. 2. Photograph from the Urseren valley showing different erosion processes (examples of landslides, livestock trails and sheet erosion are labeled). The image was taken in early summer of 2009.

While the different scientific communities have been using OBIA to map erosion features with distinct boundaries (e.g., gullies, landslides), no study known to the authors has been conducted on mapping all occurring erosion processes including diffuse boundaries (e.g., sheet erosion) in a single approach for Alpine grasslands. With this study we present a holistic approach using OBIA to identify all visible occurring processes causing soil loss on Alpine grasslands (Urseren Valley) on high-resolution RGB orthophotos. In many cases the transitions between different types of erosion processes are not distinct, but for this study we assign classes to eroded and degraded sites according to their leading erosion type or process (shallow landslides, sheet erosion) and erosion caused by land use management (livestock trails, management effects) with a set of rules defined in Section 3.2 based on typical visual characteristics of the classes, such as spectral properties or geometric attributes.

By mapping multiple orthophotos (2000–2016) we aim at a time series that allows for a comprehensive analysis in space and time of all the erosion processes. Spatio-temporal maps will give us valuable insights into the erosion dynamics of the catchment including even small

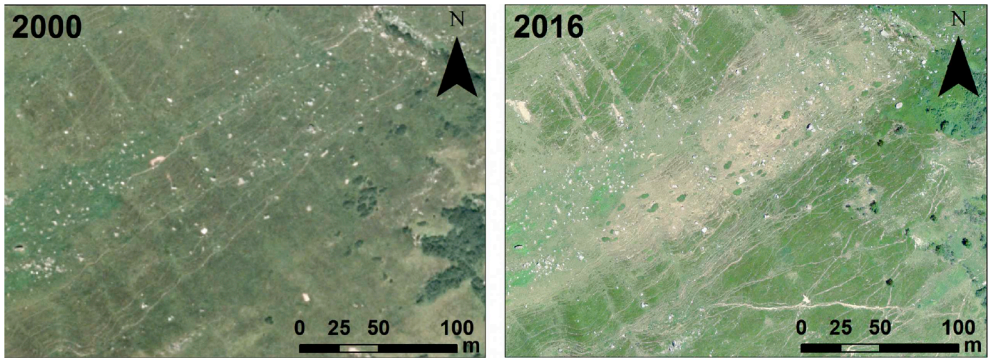

Fig. 1. Sub-image from the orthophotos of the Urseren Valley. The side by side comparison of the images taken in 2000 and 2016 show the increasing amount of soil degradation over time.

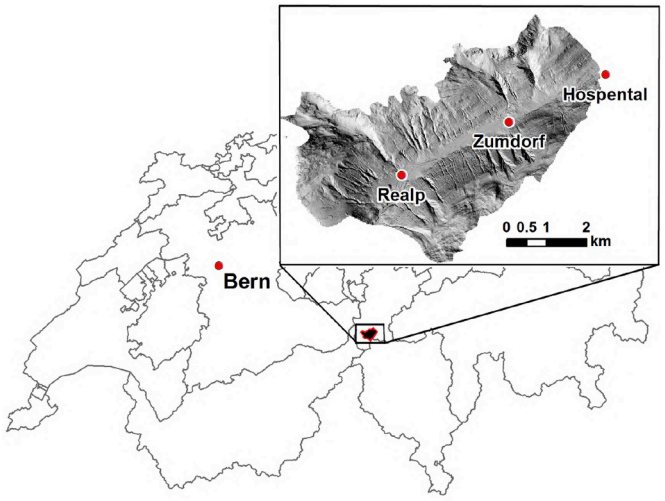

Fig. 3. The Urseren Valley and its location within Switzerland.

scale erosion features, which is crucial information for sustainable land management (Alewell et al., 2008).

2. Study area

The selected study site is located in the high-alpine Urseren Valley (Fig. 3) in the Swiss Central Alps (Canton Uri) and covers an area of 26 km^2. The valley has a mean slope angle of 27° and is discharged by the river Reuss. With elevations between 1400 and 3200 m asl the valley is exposed to subalpine-alpine climate conditions. The mean annual temperature of the nearest station (Andermatt, 1438 m asl) is 4.0°C (period 1981 to 2011) and the mean annual rainfall is 1400 mm (max. in October, min. in February). On average, the maximum yearly precipitation intensity is 110 mm/3d with values ranging up to 270 mm/3d in the year 2000 (Source MeteoSwiss). The valley is covered with snow from November until April (mean seasonal snow depth of 60 cm) with a maximum in March (mean snow depth of 95 cm) (Source MeteoSwiss). While the run-off is dominated by snow melt from May until June (max. in June), summer and autumn floods can also be major contributors to the flow regime.

The orientation of the U-shaped valley is NE–SW and is situated along a tectonic fault line separating Gneiss of the Gotthard massif on the south and Granite of the Aare massif on the north (crystalline basement called “Altkristallin” (Labhart, 1999)). Along the fault line there are vertically dipping layers consisting of Permacarbonic (sandy-clay deposits) and Mesozoic sediments. The latter consists of different material depositions from the Triassic period (sandstone, rauhwacke and dolomite), early Jurassic period (“Lias”; dark clay-marl and marl) as well as from middle Jurassic period (“Dogger”; clays, marl and limestone). During orogenesis, the material was metamorphosed to schist (Angehrn, 1996; Wyss, 1986; Kägi, 1973). The south-east facing slope contains clay-rich soils produced by weathering of the calcareous bedrock which provide a high risk for slope instabilities. The prevailing soil types in the Urseren Valley are Podzols and Cambisols (after IUSS Working Group WRB (2006)). Leptosols are common on steep slopes and on elevations above 2000 m asl (with Rendzic Leptosols on calcareous substrate). At the valley bottom clayey Gleyic Luvisols and Gleysols can be found. Due to the deforestation of the valley, started by early settlers in 1100 A.D., the slope instability is high, avalanches are frequent and therefore an increased susceptibility to soil erosion is present (Ceaglio et al., 2012; Freppaz et al., 2010; Korup and Rixen, 2014; Stanchi et al., 2014). The potential tree line is located at approximately 2150 m asl (C. Körner, personal communications). The south-east facing slope is mainly covered with grassland and is generally more productive due to the geological bedrock and therefore is more intensely used for pasturing. The north-west facing slope is less productive and covered with shrubs, mainly *Alnus viridis*.

Livestock consists primarily of cattle and sheep with a small number of goats. With an increasing number of livestock the stocking density increased over time, causing more intense use of grassland pastures. For more details on the history of the land use in the Urseren Valley see Meusburger and Alewell (2008).

Table 1
Orthophoto acquisition dates and specifications.

Year	Date	GSD	Position Accuracy
2000	24. August	0.5 m	±0.5 m
2004	09. September	0.5 m	±0.5 m
2010	20. July	0.25 m	±0.25 m
2013	01. August	0.25 m	±0.25 m
2016	20. July	0.25 m	±0.25 m

3. Materials and methods

3.1. Materials

3.1.1. Orthophotos

Orthophotos (*SwissImage*) are georeferenced aerial images produced by Swisstopo (2010) that have been corrected for the influence of the terrain and of the camera. This product covers the entire area of Switzerland and is updated every three years during the vegetated season. The images contain the visible spectral bands red, green and blue (RGB) and have a ground sample distance (GSD) of 0.5 m for older images and 0.25 m for newer images (see Table 1 for details). We used the CORINE land cover data set (EEA, 2006) (spatial resolution of 100 m) to crop the orthophotos according to the presence of grasslands in the Urseren Valley. Due to the coarse resolution of the CORINE data set precise delineation of grassland areas is not possible, however, large areas containing high alpine rock fields can successfully be excluded.

3.1.2. Additional data sets

The digital terrain model (DTM) *SwissALTI3D* (Swisstopo, 2014) has a spatial resolution of 2 m. Using *ArcGIS* (Version 10.5) we calculated the slope, aspect and standard curvature (plan and profile) from the DTM, which yield important ancillary information for the classification process. We also calculated the Excess Green index (ExG), which is a vegetation index that can be calculated from only visible spectral bands (Woebbecke et al., 1995; Mayr et al., 2016) and is calculated as follows:

$$ExG = 2g - r - b$$

where

$$r = \frac{R}{R+G+B}, \quad g = \frac{G}{R+G+B}, \quad b = \frac{B}{R+G+B}.$$

Furthermore, thematic data sets (taken from the topographic landscape model *SwissTLM3D* (Swisstopo, 2019)) containing information on the presence of roads, rivers/streams and buildings were used to refine the rule set. All above mentioned data sets are listed in Table 2.

Table 2
List of data sets used for the object-based image analysis.

Product	Description	Type	Spatial Res.
SwissImage	Orthophotos (Red, Green, Blue Bands)	Raster	0.25–0.5 m
SwissALTI3D	Digital Terrain Model; Calculated Derivatives	Raster	2 m
SwissTLM3D	Thematic Layers (Roads, Streams, Buildings)	Vector	1 : 25′000
CORINE	Land Cover (Grasslands)	Raster	100 m

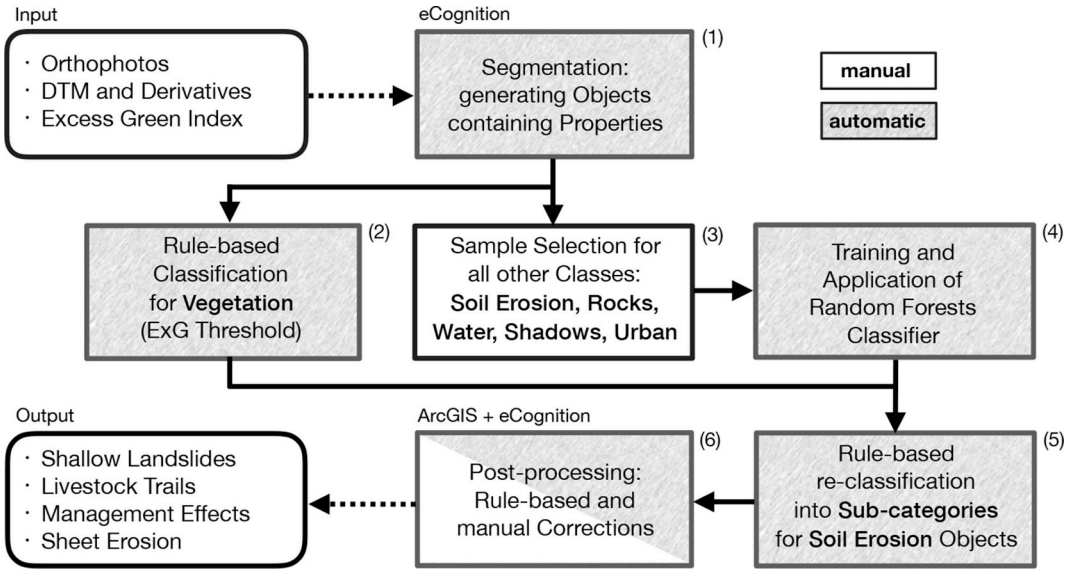

Fig. 4. Work-flow diagram of the object-based image analysis used to map and classify visible soil erosion features. Steps that require manual work are described in white boxes, while automatic steps are described in grey boxes. Numbered steps are further described in the text with (1)–(6).

3.2. Erosion mapping with object-based image analysis

To identify and map the degraded sites on the orthophotos we used OBIA. The work-flow was developed with the software *eCognition Developer* (Version 9.3.2) (Fig. 4). As a first step, object primitives are generated by grouping together pixels with similar properties (1). For the generation of the object primitives, the multi-resolution segmentation algorithm of eCognition was used (scale parameter = 40, shape = 0.1, compactness = 0.5). The segmentation takes into account the heterogeneity of pixel values (RGB) as well as the size of the desired image objects. Additionally, the DTM and its derivatives as well as the calculated ExG index were incorporated during the segmentation process. Parameters were calibrated manually, while care was taken to achieve object primitives that best represent our target objects, which show a strong variation concerning their shape as well as size.

The orthophotos of the catchment were divided into four sub-sections to better handle the data load (above and below 2000 m asl as well as south and north of the river). In a next step, a manually calibrated ExG index threshold was applied to classify all objects belonging to the class *vegetation* (2). ExG thresholds varied from one orthophoto to the next, however, ideal values were well defined. For all other unclassified objects, samples were selected to represent their class (soil erosion, rocks, shadow, water, roads or buildings) (3). For every orthophoto roughly 3% of all objects were manually selected as samples across the entire area. Approximately 30% of the samples were selected to represent the class *soil erosion*, as this class contains bare soil areas as well as patches with strongly reduced vegetation cover, which exhibits a wide variety of appearances. The selected samples were used to train the random forest classifier based on the object features listed in Table 3 to classify all remaining unclassified objects (4). For the random forest classifier, which was applied within eCognition, we selected all 36 predictors (Table 3), with 6 features considered per split with a tree size of 6 and a maximum tree number of 50, which offered the best trade-off between calculation time and classification performance. The object features used for the random forest classifier (Table 3) were selected from the point of view of differentiating soil erosion objects from all other objects (e.g. rocks, water, urban). Features consist of various layer values derived from the orthophoto, the ExG index, the DTM and its derivatives as well as geometric variables and object textural variables from the Grey Level Co-occurrence Matrix (GLCM) (Haralick et al., 1973) and were chosen based on literature (Martha et al., 2010; Moine et al., 2009; Stumpf and Kerle, 2011) and testing of further features within eCognition. Information on the feature importance results of the random forest classifier can be found in the supplementary material (Fig. S1). At this stage, the random forest classifier has classified objects belonging to the class *soil erosion*. To allocate the specific erosion sub-categories to the soil erosion objects we created an additional rule set based on the visual appearance of the four sub-categories, described in detail below. For the differentiation between the categories we translated the visual characteristics in to suitable object features and calibrated thresholds (Table 4; for more details see Table S1 in the supplemental material) (5). We distinguish between erosion classes, that are clearly identifiable with distinct boundaries, namely *shallow landslides*, *livestock trails* and *management effects*. For sites with reduced vegetation cover and diffuse boundaries we assume *sheet erosion* to be the dominant erosion process.

Shallow landslides are distinguished by their clear boundary to the surrounding vegetation as well as their relatively compact shape and occurrence on steeper slopes (> 25°) (Meusburger and Alewell, 2008; Wiegand and Geitner, 2013). Livestock trails, on the other hand, are

Table 3
List of object features used for the random forest classifier.

		Object Features
Layer Values	Mean	R, G, B, ExG, Elevation, Aspect, Slope, Curvature, Hue, Intensity, Saturation, Brightness
	Std. Dev.	R, G, B, ExG, Elevation, Aspect, Slope, Curvature
	Border Contrast	ExG
Geometry	Extent	Area, Length/Width
	Shape	Compactness, Density, Elliptic fit, Roundness, Rectangular fit, Shape Index
Texture	GLCM (all dir.)	Contrast, Dissimilarity, Entropy, Mean, Std. Dev., Correlation

Table 4
List of object features used in the rule set to define soil erosion categories.

Erosion Category	Object Features
Shallow Landslides	Mean Slope, Border Contrast of ExG, Shape Index, Rel. Border to Class 'Vegetation'
Livestock Trails	Length/Width, Density, Main Direction
Management Effects	Area, Mean Slope
Sheet Erosion	Remaining 'Soil Erosion' Objects

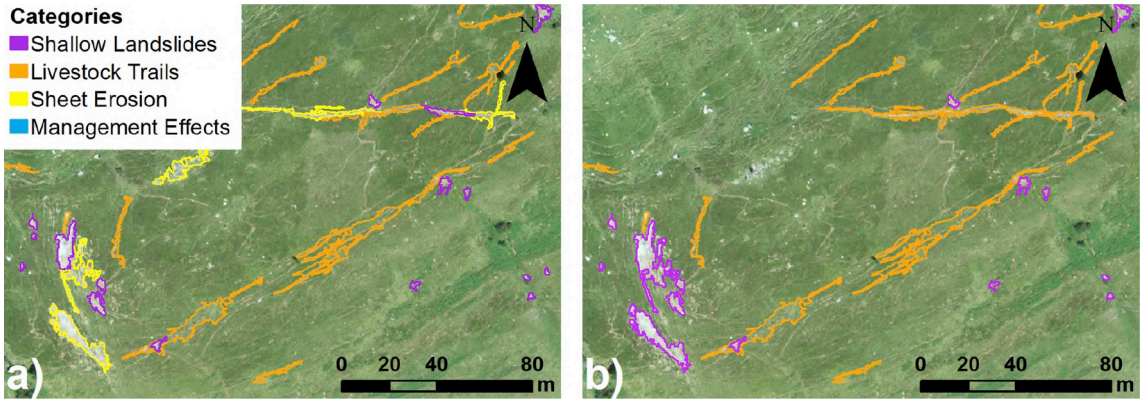

Fig. 5. A subarea of the Urseren Valley (2013) showing an example of classification results a) before and b) after manual corrections.

very uniquely elongated and narrow and follow the contour lines of the slope within a range of ± 20°. Management impacted grasslands are typically large, compact areas with distinct boundaries (e.g., within fences or ownership boundaries) and are found near the valley floor on gentle slopes (< 25°) easily accessed with machinery. Remaining objects are classified as areas with reduced vegetation cover susceptible to sheet erosion, as it is difficult to determine a certain pattern, due to the various shapes, sizes and locations of this type of erosion process.

Post-processing in the form of visual assessment and subsequent manual corrections of the results was required to assure the comparability of the erosion classes between the individual years (6) (Fig. 5). Objects with an area $< 4\ m^2$ were removed from all results to assure conformity between all years, due to the varying GSD or the orthophotos.

3.3. Verification

For all erosion classes we conducted a thorough visual investigation with zooming in to the respective orthophotos to assure the accuracy of the classification results as well as an accuracy assessment of randomly selected points. The latter was conducted with five soil experts familiar with the field situation in the valley. Each expert evaluated 100 random points for each orthophoto, generating a total of 500 points per expert. Approximately half the sample points were randomly selected from the class background and the other half from erosion classes, to best evaluate the overall accuracy of erosion classes, which occur rarely compared to background pixels. The randomly chosen pixels were independently reviewed through visual assessment and were allocated by the experts to the following classes: shallow landslides, livestock trails, sheet erosion, management effects or background (anything other than soil erosion). These results were then compared to the results of OBIA to calculate accuracy scores for each mapped orthophoto. The accuracy was assessed based on the error matrix and the related statistics, namely the Overall Accuracy, Producer's Accuracy, User's Accuracy and Kappa coefficient (Radoux and Bogaert, 2017).

Additionally, we calculated accuracy scores for shallow landslides for the two years (2000 and 2004) overlapping with the manually mapped landslides from the previous study by Meusburger and Alewell (2008) (only sites $> 10\ m^2$ to guarantee comparability). Verification with field measurements was only possible with a limited selection of random sites, due to the large extent of the study area. Due to the extreme topography and the fact that field measurements were conducted 2 years after the newest orthophoto was taken (2016), the choice of suitable erosion sites was limited. While the location and the extent of shallow landslides can clearly be determined in the field it was not possible to determine the exact boundaries of the other erosion features two years later. For the mapped shallow landslides, field measurements of ten sites were compared to the length and width of the objects generated with OBIA. The measurements of the OBIA mapped landslides were corrected for the steepness of the slope to guarantee comparability.

4. Results & discussion

4.1. Spatial distribution of mapped erosion sites

Mapping of the orthophoto taken in 2016 resulted in 3.4% of the valley surface being affected by some type of erosion process (Fig. 6). Examples of the four erosion classes and their appearance on orthophotos can be seen on Fig. 7. The south-east facing slope is more strongly affected by soil erosion and contains 92% of all mapped sites. Concurrently, grassland is the dominant vegetation cover on this side of the valley. Most agricultural activity in the form of livestock grazing and haying takes place on the lower slopes of this side due to the higher fertility of the soil developed on calcareous and silicate schists, which in turn are prone to erosion. The grassland surface area in this land use zone (< 2000 m asl) is affected by 6.8%. The north-west facing slope, on the other hand, is mostly covered with shrub vegetation (*Alnus viridis*, *Sorbus aucuparia*), and is less favored for agricultural use (Meusburger and Alewell, 2008).

Shallow landslides are commonly quite small with an average size of 40.2 m^2. They can, however, vary in size from very small (4 m^2) to 6172 m^2 for the largest site, which is located in steep terrain and caused by headward erosion of the stream. Most sites tend to be smaller but are often aggregated into groups, with 69.2% of landslides located within 10 m of each other. Additionally, landslide locations are often in close

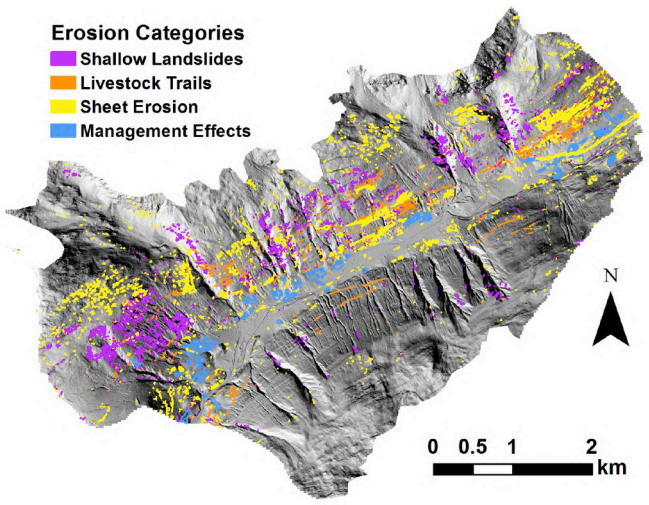

Fig. 6. The map shows the relief of the Urseren Valley with the OBIA mapped erosion sites based on the most recent orthophoto of 2016.

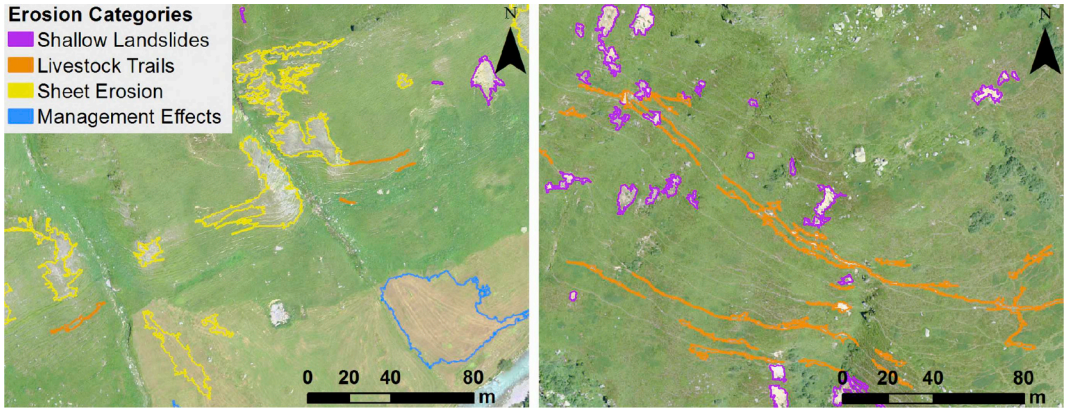

Fig. 7. Illustration of the different erosion types as they appear on the orthophoto (2016) and are subsequently mapped with OBIA.

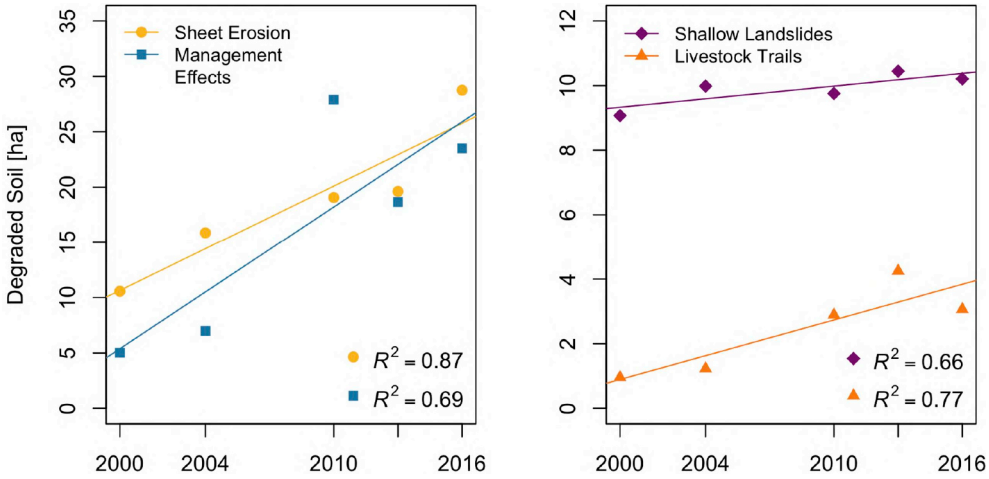

Fig. 8. Temporal development of all soil erosion classes in the Urseren Valley for each analyzed year between 2000 and 2016. Lines indicate the trend given by a linear regression.

proximity to streams, with 49.4% within a distance of 100 m. The slope angles at which shallow landslides primarily occur, range from 33 to 44° with a mean of 39°, which agrees with other studies (Blechschmidt, 1990; Rickli and Graf, 2009; Tasser et al., 2003; Wiegand and Geitner, 2013). The elevation of slopes affected by shallow landslides ranges from 1769 to 2087 m asl with a mean of 1931 m asl. The dominant slope aspects are east (43%) and south (41%) with fewer landslides located on western slopes (12%). These findings generally agree with studies conducted for other regions in the Alps, such as by Blechschmidt (1990) (Karwendel), Laatsch and Baum (1976) (Bavarian Alps) and Wiegand and Geitner (2013) (Tyrol). The south-east facing slope is exposed to more direct solar radiation and therefore experiences more snow-gliding events and enhanced snow-melt, which can trigger shallow landslides (Meusburger et al., 2013; Tasser et al., 2003; Wiegand and Geitner, 2013). Furthermore, snow-gliding is more easily triggered with wet boundary layer between the soil and snow cover, which is more likely given with warmer ground conditions (Fromm et al., 2018; Newesely et al., 2000).

Livestock trails generally follow the contour lines and occur on moderately steep slopes (26–36°), where cattle and sheep often traverse for grazing purposes. The average elevation of livestock trails is 1749 m asl and therefore are located close to the foot of the slope. There are, however, sites ranging up to 1834 m asl. The majority of livestock trails (85%) are found on the south-east facing side of the valley.

Sites with reduced vegetation cover caused by **management effects** are located near the foot of the slope (up to 1596 *m asl*) and occur on gentler slope angles (12–22°). These areas are mostly used for hay production to feed livestock during winter months (Meusburger and Alewell, 2008).

Exposed soil surfaces susceptible to **sheet erosion** (from here on referred to only as *sheet erosion*), is a phenomenon that occurs across the entire catchment on all grassland surfaces. The triggering factors for these exposed soil surfaces are not consistent. Sheet erosion sites at lower elevations are mostly in the proximity of livestock trails and are therefore connected to land use practices. The sites at higher elevations are most likely caused by precipitation and snow movement or snow melt. The shapes and sizes of the sheet erosion objects vary greatly from only 5 m^2 up to 3 ha with a mean of 117 m^2. The average slope angles of affected sites range from 17 to 36° with a mean of 27°. Thus, sheet erosion is present on gentler as well as on steeper slopes.

4.2. Spatio-temporal development

Applying the OBIA method to historical orthophotos yields a time series with irregular frequencies starting from the year 2000. From 2000 until 2016 the measured area affected by soil erosion (sum of all four erosion categories) has increased by 156 ± 18% (estimated propagated error based on accuracy assessment). This increase can be observed for all occurring erosion types with various intensities (Fig. 8).

To achieve a more comprehensive understanding of the dynamic aspect of the erosion sites, we analyzed temporal and spatial changes simultaneously. Sheet erosion and management effects have increased substantially since 2000 (from 10.30 to 28.75 ha for sheet erosion and 4.06 to 23.49 ha for management effects) with management effects

showing strong variations from 2010 to 2013. Shallow landslides and livestock trails both are generally smaller in size and also affect a smaller area. **Shallow landslides** show a constant but comparably small increase from 9.07 to 10.21 ha between 2000 and 2016. Meusburger and Alewell (2008) and Alewell et al. (2008) concluded that the amount of soil material eroded by landslides is considerably smaller than by sheet erosion. We can confirm regarding the areal effect that shallow landslides, even though being the most obvious erosion feature, are quantitatively not the dominant erosion process in the Urseren Valley. **Livestock trails** affect only a small area due to their narrow appearance but have, nevertheless, steadily increased during the investigation period (1.04-3.06 ha) with a peak in 2013 (4.25 ha). The decrease of livestock trails after 2013 is mainly due to the widening of the trails due to continuous trampling and grazing and/or climate effects which resulted in a shift into being classified as sheet erosion in 2016. The effect of livestock trails on erosion processes might be two-fold. The horizontal structuring (i.e., "terracing") of the slopes can decrease the snow-gliding distance as well as the overland flow (Alewell et al., 2015; Tasser et al., 2003). Due to this fragmentation of the grassland surface in these areas only small parts of the topsoil are able to slide off (Tasser et al., 2003). On the other hand, due to the damaged vegetation cover and soil compaction caused by livestock trampling and grazing, shallow landslides and sheet erosion can be triggered more easily by winter processes (e.g., snow-melt or snow-gliding) and strong precipitation events/water saturation of soil (Alewell et al., 2015; Dommermuth, 1995; Konz et al., 2010; Tasser et al., 2003). Our results show, that areas highly affected by livestock trails lead to increased areas with reduced vegetation cover as well as landslides over time. As such, an increased amount of livestock trails can be a triggering factor for other erosion processes.

An overall increase in sites affected by **sheet erosion** is observed for the entire catchment. However, there is a high spatial variability observed in the results for the different orthophotos. This variability is due to the fact that these areas have a reduced vegetation cover, for which it is difficult to define clear boundaries. Especially in the case of very small degradation sites mapping precision as well as repeated detection on different orthophotos with differing color characteristics (e.g., solar angle, color tones) might be impaired. Additionally, having time steps of at least three years between the orthophotos allows for recovery of sheet erosion sites as well as the development of new sites. Areas that are permanently affected by sheet erosion are located at lower elevations in areas intensively used for pasturing.

The visual appearances of **management effects**, mainly caused by the use of heavy machinery or the application of manure at unsuitable times leaving the soil bare or the vegetation cover damaged, are very variable from one year to the next. Although the trend is generally increasing, possibly due to changing land use practices, the size of the affected area is very dependent on the timing of the orthophoto. In most cases these sites recover quickly, but in the meantime the exposed areas are vulnerable to erosion.

By dividing up the amount of eroded area in to elevation sections, we can observe the changes from 2000 to 2016 by erosion class (Fig. 9). For livestock trails, sheet erosion and management effects the affected area has strongly increased at lowest elevations (1500–1750 m asl), which coincides with agricultural land use areas. For shallow landslides a shift in susceptibility zone can be observed. While higher elevations (1750–2250 m asl) show an increase, there is a small decrease at lowest elevations. This is discussed in further detail in Section 4.2.1.

4.2.1. Shallow landslides

The spatio-temporal analysis of shallow landslides is discussed in more detail, as the sites have unambiguous, clear boundaries and we were able to compare our data with a previous study of manually mapped landslides by Meusburger and Alewell (2008). The temporal analysis reveals high dynamics within the catchment (Fig. 10).

Changing areas are either highlighted as degrading (red; increasing trend) or as recovering (blue; decreasing trend). While recovery can be observed in some areas (i.e., north-east section and north-west facing slope), most grid cells show a strong increase, mainly located on the south-east facing slope. Most shallow landslides are located at mid-range elevations (1750–2000 m asl) and have increased only slightly since the year 2000 (Fig. 9). While areas near the valley bottom (1500–1750 m asl) show a minor decline, the amount of area affected by shallow landslides above 2000 m asl has increased by around 40% (1.8-3.1 ha). Affected areas near the valley floor are located in a geologically susceptible formation (Mesozoic layer) as well as regions heavily used for cattle and sheep pasturing (for more information on land use and geology see Meusburger and Alewell (2014)). The increase at higher elevations cannot be explained by intensified land use practices, as there is hardly any change in the intensity of livestock grazing. Therefore, the increase might be caused by snow processes and precipitation. Field observations at these higher sites indicate snow-gliding processes during the winter, such as abrasion marks on the bare soil and rolled up vegetation in the vicinity of shallow landslides shaped by the pressure of the moving snow cover (Meusburger and Alewell, 2014).

In addition to catchment scale overviews, the results allow for close-up evaluations of sites for better understanding of the local dynamic impacts on degraded sites (Fig. 11). In the depicted region, a triggering event between the years 2010 and 2013 caused a sudden increase of bare soil sites. The disappearance of shrubs might have been caused by a high intensity event, such as an avalanche, or an increase in sheep stocking, as sheep for debarking shrubs (e.g., *Alnus viridis*, *Sorbus aucuparia*) were introduced to the valley for landscaping purposes.

As the two orthophotos of 2000 and 2004 were also used in the study by Meusburger and Alewell (2008), we compare results of manually mapped sites with results of OBIA (Fig. 12). Because OBIA is capable of mapping smaller landslides ($>4\ m^2$) than the manual method allows ($>10\ m^2$), the total area is slightly higher for both years we compare (1.1 ha more on average). Still, the increasing trends are comparable between the two methods. The area affected by shallow

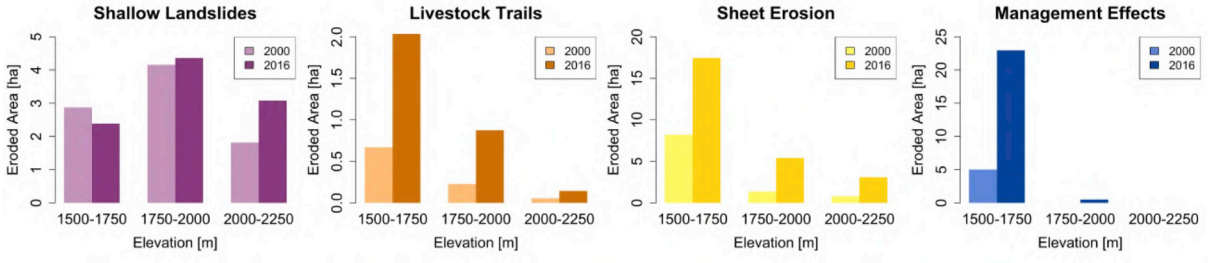

Fig. 9. Susceptibility zones with changes observed from 2000 to 2016 for shallow landslides (purple), livestock trails (orange), sheet erosion (yellow) and management effects (blue). Scales of the x-axis vary between erosion classes. (For interpretation of the references to color in this figure legend, the reader is referred to the Web version of this article.)

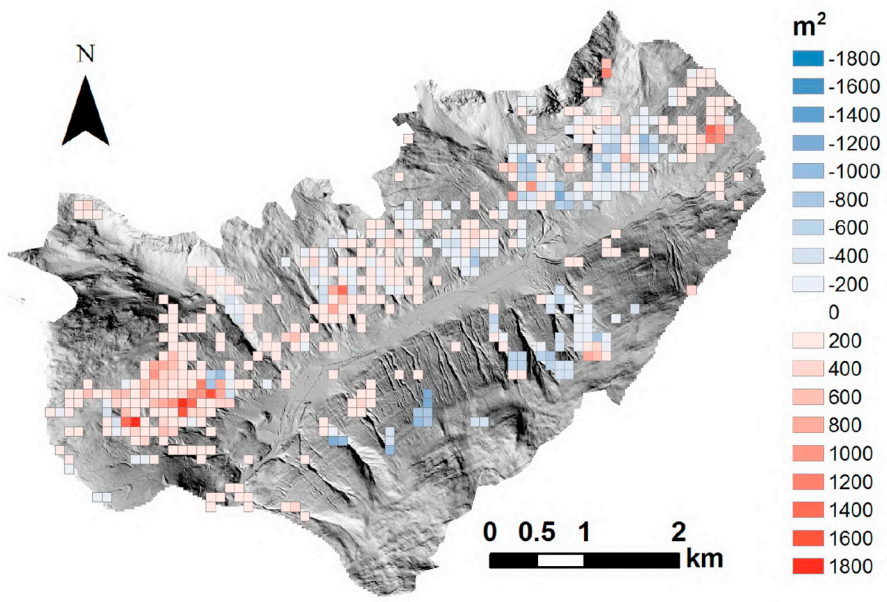

Fig. 10. The Urseren Valley with its temporal and spatial changes of shallow landslide affected areas between 2000 and 2016. Grid-cells have a size of 100×100 m. Areas in blue show amount of decrease and areas in red show amount of increase. (For interpretation of the references to color in this figure legend, the reader is referred to the Web version of this article.)

landslides has doubled since 1959 from approx. 5 to 10 ha, demonstrating that long term monitoring is a necessity, as recovering phases are succeeded by newly triggering events.

4.3. Possible causes for increasing trends in soil degradation

Our results show an increase for all erosion types during the study period. Meusburger and Alewell (2008) showed that shallow landslides specifically have increased over a longer time period using images dating back to 1959. Some factors influencing soil degradation and soil erosion can be considered constant over time, such as the geological bedrock or the topographical conditions. However, other factors influencing erosion processes undergo dynamic changes, such as climate conditions and land use management. We found that areas of the Urseren Valley at lower elevations are showing increasing amount of erosion including erosion patterns linked to anthropogenic activity, such as land use management. Regions at higher elevations are barely used for agricultural purposes and therefore the observed increase has to be linked to climate related factors or grassland abandonment (Tasser et al., 2003; Meusburger and Alewell, 2008). Heavy machinery was introduced in the 1970's which simultaneously replaced traditional farming (e.g., manually repairing spots of damaged soil surface, cutting back single shrubs etc.) (Meusburger and Alewell, 2008; Scheurer et al., 2009). We have been able to document this increase in observable management degradation on the lower slopes using OBIA. These management changes also influenced the use of livestock pastures. While remote and difficult to access areas were abandoned due to the resignation of permanent herding practices, areas closer to the valley floor and therefore easier to access, are being used more intensely (Meusburger and Alewell, 2008). In addition to a decrease in the effective pasture areas (i.e., because higher alpine pastures were abandoned), the number of cattle and sheep was increased (Meusburger and Alewell, 2008). These changes coincide with the increased amount of livestock trails observed and mapped at lower elevations, and may still have a continuous affect in the future. Sheet erosion is caused by increased run-off and/or by a reduction of the vegetation cover (Meusburger and Alewell, 2014; Nearing et al., 2004). The vegetation cover can be damaged by grazing and trampling of livestock or biomass production can be affected by drought. The latter can cause hydrophobicity and sealing of the soil and thereby changes run-off properties (Konz et al., 2010; Nearing et al., 2004; Scheurer et al., 2009). Presently, there are more days in the summer without rain, and this is expected to continue in the future. However, extreme precipitation events will be more frequent, which has already been observed for many areas in Switzerland since 1901 (CH2018, 2018). Prolonged intense precipitation events are also a major cause of shallow landslides

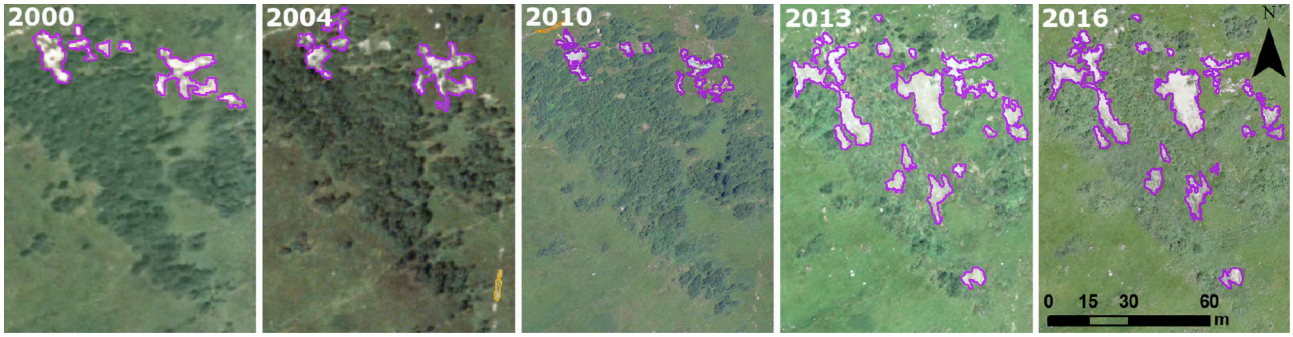

Fig. 11. A selected subset of the Urseren Valley as an example for the dynamic aspect of erosion on grasslands. The time series shows the evolution of shallow landslides from 2000 to 2016 parallel to a decrease in shrub cover. The smallest detected objects have a size of 4.5 m^2.

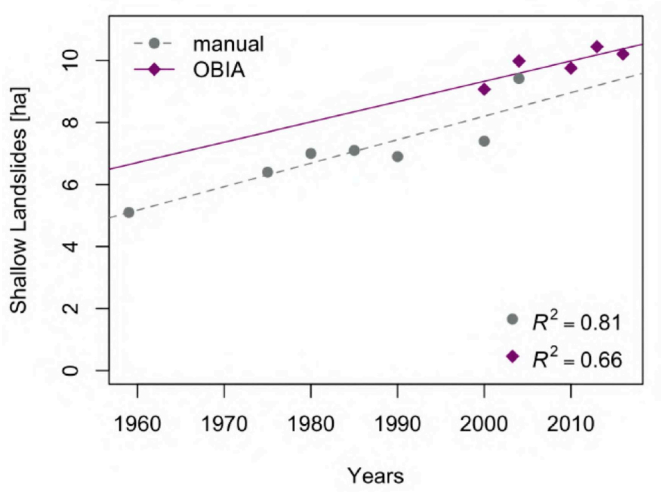

Fig. 12. Urseren Valley showing the temporal development of shallow landslides between 1959–2016 of the total affected area. Grey points (1959–2004) were mapped manually by Meusburger and Alewell (2008) and purple points (2000–2016) were mapped using OBIA. Lines indicate the trend given by a linear regression. (For interpretation of the references to color in this figure legend, the reader is referred to the Web version of this article.)

(Gariano and Guzzetti, 2016). An increasing temperature trend has been observed for winter months too, and is expected to increase in the future (CH2018, 2018). Rapid snow-melt with warmer spring temperatures, causes additional run-off threat to soils (Konz et al., 2012; Saez et al., 2013). The winter temperatures could also have an influence on the occurrence of snow-gliding, which is the most common cause of shallow landslides (Wiegand and Geitner, 2013). Fromm et al. (2018) found, that parameters such as higher soil temperatures and higher soil moisture contents cause increased snow-gliding. Snow movement can also produces fissures, that can lead to the formation of new landslides (Blechschmidt, 1990; Leitinger et al., 2008; Meusburger and Alewell, 2009; Wiegand and Geitner, 2010b; Newesely et al., 2000). The effects of climate change on erosion processes can be complex due to feedback mechanisms. However, with the effects of both longer dry phases and extreme precipitation events as well as altered snow dynamics we can expect more soil degradation to occur, which is consistent with our observed trends (Nearing et al., 2004; Pruski and Nearing, 2002; Saez et al., 2013; Wood et al., 2016).

4.4. Accuracy assessment

For all erosion classes we conducted a thorough visual investigation with zooming in to the respective orthophotos to assure the accuracy of the results. The analysis showed, that for livestock trails, sheet erosion and management effects the degraded areas are underestimated. For this reason, values of areas affected by these three erosion classes are to be considered as conservative estimations, with real numbers being considerably higher. Visual assessments of the orthophotos confirmed our general increasing trends of soil degradation. Additional accuracy assessment was conducted on the basis of randomly selected points, which were evaluated by experts familiar with the field situation in the valley (see Section 3.3). The evaluated points were compared to the results of OBIA to calculate accuracy scores for each mapped orthophoto (Table 5). The Overall Accuracy is in a range of 0.78 to 0.88 for all orthophotos with Kappa coefficients ranging from 0.65 to 0.81. Lower scores were achieved for the year 2004, which also has the darkest color conditions and was therefore harder to work with. With similar scores for the year 2000 compared to newer images (2010, 2013, 2016), we can assume, that the lower spatial resolution does not have major impacts on the accuracy of the results.

Table 5
Accuracy scores of erosion categories using random sample evaluation.

Orthophoto	Overall Acc.	Producer's Acc.	User's Acc.	Kappa
2000	0.87	0.77	0.79	0.81
2004	0.78	0.62	0.64	0.65
2010	0.88	0.86	0.85	0.81
2013	0.87	0.82	0.85	0.80
2016	0.87	0.89	0.81	0.81

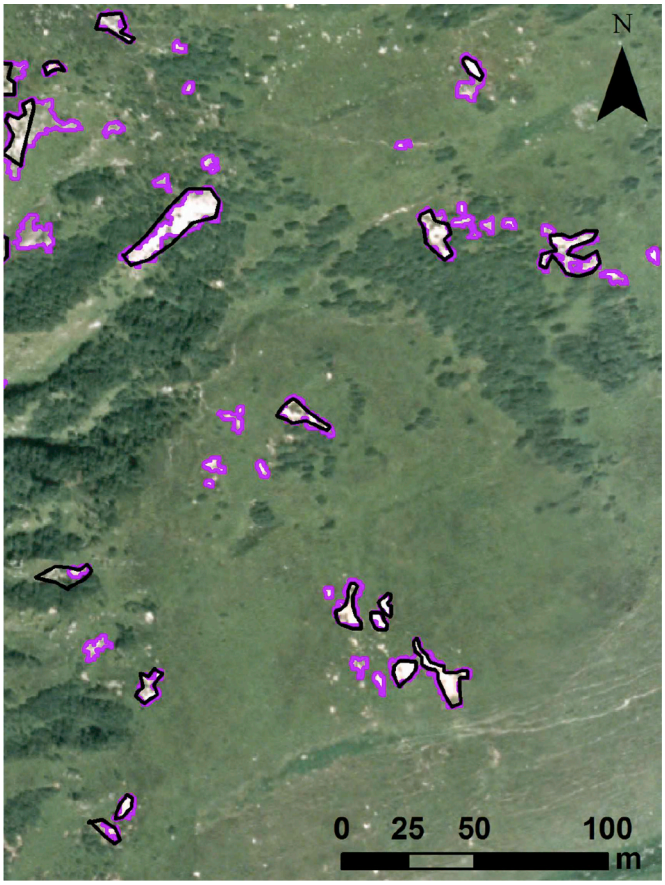

Fig. 13. A subarea of the Urseren Valley (2000) showing the results of the OBIA classification (purple) vs. the manual classification (black) of shallow landslides produced by Meusburger and Alewell (2008). (For interpretation of the references to color in this figure legend, the reader is referred to the Web version of this article.)

With OBIA we generally obtain more accurate boundaries of erosion features and also detect smaller sites, which are mostly missed during manual mapping (Fig. 13). Nevertheless, we also compared the shallow landslides of the manual data set to our OBIA results (only sites $> 10\ m^2$ to guarantee comparability) and calculated accuracy measures based on overlapping objects for the years 2000 and 2004. The OBIA mapped landslides have a Producer's Accuracy of 0.91 and a User's Accuracy of 0.86, which coincide with visual assessments, that landslides are the erosion features with the highest mapping accuracy. Additional measurements in the field showed, that the mean areal deviation between measurements and their corresponding sites mapped with OBIA is 6.5%.

4.5. Limitations of the method

The investigation of the results showed, that the quality of mapped shallow landslides is very satisfying (Section 4.4). The other erosion classes have boundaries that are difficult to precisely delimit due to

smooth transitions (sites with reduced vegetation cover susceptible to sheet erosion) or are simply too fine to always capture their entirety (livestock trails). The lower spatial resolution of 0.5 m of the orthophotos taken in 2000 and 2004 makes the precise erosion mapping more difficult, especially in the case of livestock trails. Even though features with clear boundaries $> 4\ m^2$ were detected, the overall area mapped as degradation is rater underestimated due to (i) underestimation of feature area or (ii) non-detection of features with very diffuse boundaries. Other issues we encountered were the varying color spectra of the orthophotos mainly caused by the different acquisition times. This had a significant effect on the color of the vegetation, which required adaptations of the OBIA work-flow concerning ExG thresholds and some color related features such as brightness. Additional manual corrections were necessary to assure the correct mapping with OBIA and to guarantee the comparability between the individual years (Fig. 5). For certain years up to 20% of soil erosion object classifications had to be changed manually after applying OBIA. Re-classifications mainly consisted of changing sheet erosion to shallow landslides and vice versa, to match mapping results of preceding orthophotos. Another source of error were individual rocks, which were not always successfully excluded from the soil erosion objects during the random forest classification. In some cases it was not possible to select perfect thresholds for the rule set, which assigned one of the four specific erosion categories to the soil erosion objects. In these cases the objects were wrongly classified as sheet erosion before manual corrections, as this is the remaining erosion class by default. The work time to map one orthophoto was approximately 4-5 working days including manual corrections.

5. Conclusions & outlook

For this study, we developed a holistic approach using OBIA to provide information on the location and extent of different erosion features on high-resolution orthophotos (0.25–0.5 m) for the Urseren Valley (Central Swiss Alps). We were able to use OBIA to map and classify sites according to the main erosion process or triggering land use management impact. For this purpose, we differentiate between erosion sites with clear boundaries (shallow landslides $> 4\ m^2$, livestock trails or management effects) and degraded sites with more diffuse boundaries (sites with reduced vegetation cover susceptible to sheet erosion). The differentiation between soil erosion class as well as the possibility to map small erosion features is crucial for the understanding of ongoing soil degradation within the catchment as well as for decision making at the level of local authorities to determine suitable land use and mitigation possibilities.

Our results show that soil degradation has increased during the study period for all erosion classes. The south-east facing slope, which has a higher fertility and therefore is used more intensely for pasturing, is affected by 90% of the ongoing soil degradation. We found that an increase of soil degradation at lower elevations is mainly due to land use practices, as increases were primarily classified as livestock trails, sheet erosion and management effects. Slopes at higher elevations, however, which are not or only to a limited extent used for grazing purposes are mostly affected by an increasing amount of shallow landslides and sheet erosion, that we associate with changing climate conditions (e.g., more frequent precipitation events, prolonged drought and changing snow dynamics).

Verification and corrections of the results are labor intensive and affected areas are often only conservative estimates due to the limiting factor of the spatial resolution of the images used. The results of the mapped erosion categories have Overall Accuracy scores of 0.78–0.88 (Kappa of 0.65–0.81). The date of acquisition of the orthophotos (e.g., color or state of the vegetation) and temporal variability of erosion processes are the main challenges for the mapping procedure. Especially fine erosion features, such as livestock trails, are often difficult to map in their entirety, due to the spatial resolution of the images. Small erosion sites are generally more difficult to detect repeatedly from one year to the next, due to the dynamic nature of these erosion sites, which also includes recovery of affected areas.

Spatial resolutions of orthophotos and digital terrain models are expected to increase in the future with SwissImage already being produced with a GSD of 10 cm for certain regions in Switzerland. These improvements in data quality will increase the capability of OBIA mapping. Not only will finer objects become easier to classify, but also the textural information used during the analysis is likely to improve. Furthermore, including more spectral bands, such as near infrared, would increase classification accuracy. Although this data is available (e.g., SwissImage RS containing RGB and NIR channels), no historical data set exists yet, which was an essential limitation for this study. OBIA has proven to be a powerful tool for mapping erosion on catchment scale and allowed us to achieve a comprehensive understanding of the ongoing soil degradation situation in the Urseren Valley. The method allows for a better understanding of the different causes leading to soil erosion as well as the resilience of the soils. The method is transferable to other regions of similar scale, with slight adaptations to the work-flow concerning local conditions, such as the aspect of slopes in the valley (e.g., for the direction of livestock trails or color conditions of the images). However, the labor intensity of OBIA likely hinders efficient up-scaling of research areas to regional, national or continental scale. As such, for large-scale studies alternative methods such as Deep Learning might be considered for the detection and classification of objects on remotely sensed images.

Declaration of competing interest

The authors declare no conflict of interest.

Acknowledgements

This study was funded by the Swiss National Science Foundation (Project No. 167333) as part of the National Research Program *NRP75 - Big Data*. We want to acknowledge Geodata4edu and MeteoSwiss for providing the data sets we used. Additionally, we are very thankful to the anonymous reviewers for their valuable suggestions and comments with which this paper was improved.

Appendix A. Supplementary data

Supplementary data to this article can be found online at https://doi.org/10.1016/j.rse.2019.111441.

References

Alewell, C., Borrelli, P., Meusburger, K., Panagos, P., 2019. Using the USLE: chances, challenges and limitations of soil erosion modelling. Int. Soil Water Cons. Res. 7, 203–225.
Alewell, C., Egli, M., Meusburger, K., 2015. An attempt to estimate tolerable soil erosion rates by matching soil formation with denudation in Alpine grasslands. J. Soils Sediments 15, 1383–1399.
Alewell, C., Meusburger, K., Brodbeck, M., Bänninger, D., 2008. Methods to describe and predict soil erosion in mountain regions. Landsc. Urban Plan. 88, 46–53.
Angehrn, P., 1996. Hydrogeologische Grundlagen - Urserental. Geologisches Büro Dr. P. Angehrn AG im Auftrag von. Amt für Umweltschutz - Abteilung Gewässerschutz, Altdorf.
Apollo, M., Andreychouk, V., Bhattarai, S.S., 2018. Short-term impacts of livestock grazing on vegetation and track formation in a high mountain environment: a case study from the Himalayan Miyar Valley (India). Sustainability 10, 1–17.
Beniston, M., 2006. Mountain weather and climate: a general overview and a focus on climatic change in the Alps. Hydrobiologica 562, 3–16.
Beniston, M., 2012. Is snow in the Alps receding or disappearing? WIREs Clim. Change 3, 349–358.
Blaschke, T., 2010. Object based image analysis for remote sensing. ISPRS J. Photogrammetry Remote Sens. 65, 2–16.
Blechschmidt, G., 1990. Die Blaikenbildung im Karwendel. Jahrb. Ver. Schutz Bergwelt 55, 31–45.
Bosco, C., Rusco, E., Montanarella, L., Panagos, P., 2009. Soil erosion in the Alpine area: risk assessment and climate change. Studi Trent. Sci. Nat. 85, 117–123.

Ceaglio, E., Meusburger, K., Freppaz, M., Zanini, E., Alewell, C., 2012. Estimation of soil redistribution rates due to snow cover related processes in a mountainous area (Valle d'Aosta, NW Italy). Hydrol. Earth Syst. Sci. 16, 517–528.
CH2011, 2011. Swiss Climate Change Scenarios CH2011. C2SM, MeteoSwiss, ETH, NCCR Climate, and OcCC, Zurich.
CH2018, 2018. Climate Scenarios for Switzerland CH2018. National Centre for Climate Services, Zurich.
Chen, G., Weng, Q., Hay, G.J., He, Y., 2018. Geographic object-based image analysis (GEOBIA): emerging trends and future opportunities. GIScience Remote Sens. 55, 159–182.
D'Oleire-Oltmanns, S., Marzolff, I., Tiede, D., Blaschke, T., 2014. Detection of gully-affected areas by applying object-based image analysis (OBIA) in the region of Taroudannt, Morocco. Remote Sens. 6, 8287–8309.
Dommermuth, C., 1995. Beschleunigte Bodenabtragungsvorgänge in der Kulturlandschaft des Nationalparks Berchtesgaden. Ursachen und Auswirkungen aufgezeigt am Beispiel des Jennergebiets. Forstwiss. Centralbl. (Hamb.) 144, 285–292.
EEA, 2006. CORINE land cover (CLC). URL. https://land.copernicus.eu/pan-european/corine-land-cover/clc-2006.
Eisank, C., Hölbling, D., Friedl, B., Chin, Y., 2014. Expert knowledge for object-based landslide mapping in Taiwan. South-Eastern Eur. J. Earth Observ. 3, 347–350.
Frei, P., Kotlarski, S., Liniger, M.A., Schär, C., 2018. Future snowfall in the Alps: projections based on the EURO-CORDEX regional climate models. Cryosphere 12, 1–24.
Freppaz, M., Godone, D., Filippa, G., Maggioni, M., Lunardi, S., Williams, M.W., Zanini, E., 2010. Soil erosion caused by snow avalanches: a case study in the Aosta Valley (NW Italy). Arctic Antarct. Alpine Res. 42, 412–421.
Fromm, R., Baumgärtner, S., Leitinger, G., Tasser, E., Höller, P., 2018. Determining the drivers for snow gliding. Nat. Hazards Earth Syst. Sci. 18, 1891–1903.
Gariano, S.L., Guzzetti, F., 2016. Landslides in a changing climate. Earth Sci. Rev. 162, 227–252.
Guzzetti, F., Mondini, A.C., Cardinali, M., Fiorucci, F., Santangelo, M., Chang, K.T., 2012. Landslide inventory maps: new tools for an old problem. Earth Sci. Rev. 112, 42–66.
Haralick, R., Shanmugan, K., Dinstein, I., 1973. Textural features for image classification. IEEE Trans. Syst. Man Cybern. Syst. 3, 610–621.
Hölbling, D., Betts, H., Spiekermann, R., Phillips, C., 2016a. Identifying spatio-temporal landslide hotspots on North Island, New Zealand, by analyzing historical and recent aerial photography. Geosciences 6, 48.
Hölbling, D., Betts, H., Spiekermann, R., Phillips, C., 2016b. Semi-automated landslide mapping from historical and recent aerial photography. In: Proc. 19th Agile 2016 Conf. Geographic Information Science, Helsinki, pp. 14–17.
Hölbling, D., Eisank, C., Albrecht, F., Vecchiotti, F., Friedl, B., Weinke, E., Kociu, A., 2017. Comparing manual and semi-automated landslide mapping based on optical satellite images from different sensors. Geosciences 7, 37.
Hölbling, D., Friedl, B., Eisank, C., 2015. An object-based approach for semi-automated landslide change detection and attribution of changes to landslide classes in northern Taiwan. Earth Sci. India 8, 327–335.
IUSS Working Group WRB, 2006. World Reference Base for Soil Resources. Rome.
Johansen, K., Taihei, S., Tindall, D., Phinn, S., 2012. Object-based monitoring of gully extent and volume in North Australia using lidar data. SAVE Proc. 168–173 4th GEOBIA I.
Kägi, H., 1973. Die traditionelle Kulturlandschaft im Urserental: Beitrag zur alpinen Kulturgeographie. Ph.D. thesis, University of Zurich, Switzerland.
Karami, A., Khoorani, A., Noohegar, A., Shamsi, S.R.F., Moosavi, V., 2015. Gully erosion mapping using object-based and pixel-based image classification methods. Environ. Eng. Geosci. 21, 101–110.
Konz, N., Baenninger, D., Konz, M., Nearing, M., Alewell, C., 2010. Process identification of soil erosion in steep mountain regions. Hydrol. Earth Syst. Sci. 14, 675–686.
Konz, N., Prasuhn, V., Alewell, C., 2012. On the measurement of alpine soil erosion. Catena 91, 63–71.
Korup, O., Rixen, C., 2014. Soil erosion and organic carbon export by wet snow avalanches. Cryosphere 8, 651–658.
Laatsch, W., Baum, U., 1976. Faktoren der Wald- und Bodenzerstörung durch Schnee in den Alpen. Agrochimica 20, 324–338.
Labhart, T., 1999. Planbeilage: Geologisch-tektonische Übersichtskarte Aaremassiv, Gotthardmassiv und Tavetscher Zwischemassiv.
Leitinger, G., Peter, H., Tasser, E., Walde, J., Tappeiner, U., 2008. Development and validation of a spatial snow-glide model. Ecol. Model. 211, 363–374.
Maag, S., Nösberger, J., Lüscher, A., 2001. Mögliche Folgen einer Bewirtschaftungsaufgabe von Wiesen und Weiden im Berggebiet Ergebnisse des Komponentenprojektes D, Polyprojekt PRIMALP. Graslandwissenschaften, ETH Zurich.
Martha, T.R., Kerle, N., Jetten, V., van Westen, C.J., Kumar, K.V., 2010. Characterising spectral, spatial and morphometric properties of landslides for semi-automatic detection using object-oriented methods. Geomorphology 116, 24–36.
Martha, T.R., Kerle, N., van Westen, C.J., Jetten, V., Vinod Kumar, K., 2012. Object-oriented analysis of multi-temporal panchromatic images for creation of historical landslide inventories. ISPRS J. Photogrammetry Remote Sens. 67, 105–119.
Mayr, A., Rutzinger, M., Bremer, M., Geitner, C., 2016. Mapping eroded areas on mountain grassland with terrestrial photogrammetry and object-based image analysis. ISPRS Annals Photogramm. Remote Sens. Spat. Inf. Sci. III-5, 137–144.
Meusburger, K., Alewell, C., 2008. Impacts of anthropogenic and environmental factors on the occurrence of shallow landslides in an alpine catchment (Urseren Valley, Switzerland). Nat. Hazards Earth Syst. Sci. 8, 509–520.
Meusburger, K., Alewell, C., 2009. On the influence of temporal change on the validity of landslide susceptibility maps. Nat. Hazards Earth Syst. Sci. 9, 1495–1507.
Meusburger, K., Alewell, C., 2014. Soil Erosion in the Alps. vol. 118 Federal Office for the Environment FOEN.
Meusburger, K., Leitinger, G., Mabit, L., Mueller, M.H., Alewell, C., 2013. Impact of snow gliding on soil redistribution for a sub-alpine area in Switzerland. Hydrol. Earth Syst. Sci. Discuss. 10, 9505–9531.
Moine, M., Puissant, A., Malet, J.-P., 2009. Detection of landslides from aerial and satellite images with a semi-automatic method. Application to the Barcelonette basin (Alpes-de-Haute-Provence, France). In: Int. Conf. 'Landslide Processes: from Geomorphological Mapping to Dynamic Modelling', pp. 63–68.
Nearing, M., Pruski, F., O'Neal, M., 2004. Expected climate change impacts on soil erosion rates: a review. J. Soil Water Conserv. 59, 43–50.
Nearing, M.A., Xie, Y., Liu, B., Ye, Y., 2017. Natural and anthropogenic rates of soil erosion. Int. Soil Water Cons. Res. 5, 77–84.
Newesely, C., Tasser, E., Spadinger, P., Cernusca, A., 2000. Effects of land-use changes on snow gliding processes in alpine ecosystems. Basic Appl. Ecol. 1, 61–67.
Pruski, F.F., Nearing, M.A., 2002. Climate-induced changes in erosion during the 21st century for eight U.S. locations. Water Resour. Res. 38, 1–11.
Radoux, J., Bogaert, P., 2017. Good practices for object-based accuracy assessment. Remote Sens. 9, 1–23.
Rickli, C., Graf, F., 2009. Effects of forests on shallow landslides – case studies in Switzerland. For. Snow Landsc. Res. 82, 33–44.
Saez, J.L., Corona, C., Stoffel, M., Berger, F., 2013. Climate change increases frequency of shallow spring landslides in the French Alps. Geology 41, 619–622.
Schauer, T., 1975. Die blaikenbildung in den alpen. Schr.reihe bayer. Landesamtes Wasserwirt 1, 29.
Scheurer, K., Alewell, C., Bänninger, D., Burkhardt-holm, P., 2009. Climate and land-use changes affecting river sediment and brown trout in alpine countries - a review. Environ. Sci. Pollut. Res. 16, 232–242.
Shruthi, R.B., Kerle, N., Jetten, V., Stein, A., 2014. Object-based gully system prediction from medium resolution imagery using random forests. Geomorphology 216, 283–294.
Shruthi, R.B.V., Kerle, N., Jetten, V., 2011. Object-based gully feature extraction using high spatial resolution imagery. Geomorphology 134, 260–268.
Shruthi, R.B.V., Kerle, N., Jetten, V., Abdellah, L., Machmach, I., 2015. Quantifying temporal changes in gully erosion areas with object oriented analysis. Catena 128, 262–277.
Stanchi, S., Freppaz, M., Ceaglio, E., Maggioni, M., Meusburger, K., Alewell, C., Zanini, E., 2014. Soil erosion in an avalanche release site (Valle d'Aosta: Italy): towards a winter factor for RUSLE in the Alps. Nat. Hazards Earth Syst. Sci. 14, 1761–1771.
Stumpf, A., Kerle, N., 2011. Object-oriented mapping of landslides using random forests. Remote Sens. Environ. 115, 2564–2577.
Swisstopo, 2010. Swissimage. Das digitale Farborthophotomosaik der Schweiz.
Swisstopo, 2014. SwissALTI3D. Das hoch aufgelöste Terrainmodell der Schweiz.
Swisstopo, 2019. SwissTLM3D. Das grossmassstäbliche Topografische Landschaftsmodell der Schweiz.
Tasser, E., Mader, M., Tappeiner, U., 2003. Effects of land use in alpine grasslands on the probability of landslides. Basic Appl. Ecol. 4, 271–280.
Tasser, E., Tappeiner, U., 2002. Impact of land use changes on mountain vegetation. Appl. Veg. Sci. 5, 173–184.
Wiegand, C., Geitner, C., 2010a. Flachgründiger abtrag auf Wiesen- und Weideflächen in den Alpen (Blaiken) - wissensstand, Datenbasis und Forschungsbedarf. Mittl. Osterreichischen Geogr. Ges. 152, 130–162.
Wiegand, C., Geitner, C., 2010b. Shallow Erosion in Grassland Areas in the Alps. What We Know and what We Need to Investigate Further. pp. 76–83.
Wiegand, C., Geitner, C., 2013. Investigations into the distribution and diversity of shallow eroded areas on steep grasslands in Tyrol (Austria). Erdkunde 67, 325–343.
Wiegand, C., Rutzinger, M., Heinrich, K., Geitner, C., 2013. Automated extraction of shallow erosion areas based on multi-temporal ortho-imagery. Remote Sens. 5, 2292–2307.
Woebbecke, D.M., Meyer, G.E., Von Bargen, K., Mortensen, D.A., 1995. Color indices for weed identification under various soil, residue, and lighting conditions. Trans. ASAE (Am. Soc. Agric. Eng.) 38, 259–269.
Wood, J.L., Harrison, S., Turkington, T.A.R., Reinhardt, L., 2016. Landslides and synoptic weather trends in the European Alps. Clim. Change 136, 297–308.
Wyss, R., 1986. Die Urseren-Zone - lithostratigraphie und Tektonik. Eclogae Geol. Helv. 79, 731–767.